Monthly Notices
of the
ROYAL ASTRONOMICAL SOCIETY

MNRAS **452,** 4195–4202 (2015) doi:10.1093/mnras/stv1565

Early optical follow-up of the nearby active star DG CVn during its 2014 superflare

M. D. Caballero-García,[1⋆] V. Šimon,[1,2] M. Jelínek,[3] A. J. Castro-Tirado,[3,4] A. Cwiek,[5] A. Claret,[3] R. Opiela,[6] A. F. Żarnecki,[7] J. Gorosabel,[3,8,9†] S. R. Oates,[3] R. Cunniffe,[3] S. Jeong,[3,10] R. Hudec,[1,2] V. V. Sokolov,[11] D. I. Makarov,[11] J. C. Tello,[3] O. Lara-Gil,[3] P. Kubánek,[12] S. Guziy,[13] J. Bai,[14] Y. Fan,[14] C. Wang[14] and I. H. Park[10]

[1] *Faculty of Electrical Engineering, Czech Technical University in Prague, Technická 2, CZ-166 27 Praha 6, Czech Republic*
[2] *Astronomical Institute, Academy of Sciences of the Czech Republic, CZ-251 65 Ondřejov, Czech Republic*
[3] *Instituto de Astrofísica de Andalucía (IAA-CSIC), PO Box 03004, E-18080 Granada, Spain*
[4] *Unidad Asociada Departamento de Ingeniería de Sistemas y Automática, E.T.S. de Ingenieros Industriales, Universidad de Málaga, E-29071 Malaga, Spain*
[5] *National Centre for Nuclear Research, Hoża 69, PL-00-681 Warsaw, Poland*
[6] *Center for Theoretical Physics of the Polish Academy of Sciences, Al. Lotnikow 32/46, PL-02-668 Warsaw, Poland*
[7] *Faculty of Physics, University of Warsaw, Pasteura 5, PL-02-093 Warszawa, Poland*
[8] *Asociada Grupo Ciencia Planetarias UPV/EHU-IAA/CSIC, Departamento de Física Aplicada I, E.T.S. Ingeniería, Universidad del País Vasco UPV/EHU, Alameda de Urquijo s/n, E-48013 Bilbao, Spain*
[9] *Ikerbasque, Basque Foundation for Science, Alameda de Urquijo 36-5, E-48008 Bilbao, Spain*
[10] *Department of Physics, Sungkyunkwan University, Suwon 440-746, Korea*
[11] *Special Astrophysical Observatory of R.A.S., Karachai-Cherkessia, Nizhnij Arkhyz 369167 Russia*
[12] *Fyzikální ústav AV CŽR, v. v. i. Na Slovance 1999/2, CZ-182 21 Praha 8, Czech Republic*
[13] *Nikolaev National University, Nikolska 24, Nikolaev, UA-54030, Ukraine*
[14] *Yunnan Astronomical Observatory, Chinese Academy of Sciences, Kunming 650011, Yunnan, China*

Accepted 2015 July 10. Received 2015 July 10; in original form 2015 April 1

ABSTRACT

DG Canum Venaticorum (DG CVn) is a binary system in which one of the components is an M-type dwarf ultrafast rotator, only three of which are known in the solar neighbourhood. Observations of DG CVn by the *Swift* satellite and several ground-based observatories during its superflare event on 2014 allowed us to perform a complete hard X-ray–optical follow-up of a superflare from the red-dwarf star. The observations support the fact that the superflare can be explained by the presence of (a) large active region(s) on the surface of the star. Such activity is similar to the most extreme solar flaring events. This points towards a plausible extrapolation between the behaviour from the most active red-dwarf stars and the processes occurring in the Sun.

Key words: line: formation – stars: activity – stars: flare – gamma-rays: stars.

1 INTRODUCTION

On 2014 April 23, at 21:07:08 UT one of the stars from DG Canum Venaticorum (DG CVn) flared bright enough (300 milliCrab in the 15–150 keV band) to trigger the *Swift* satellite's (Gehrels et al. 2004) Burst Alert Telescope (BAT; Barthelmy et al. 2005). Within two minutes of this T_0, *Swift* had slewed to point its narrow-field telescopes to the source, which revealed gradually decreasing soft X-ray emissions with a second weaker flare occurring at $T_0 + 11$ ks, followed by several smaller flares. This behaviour was observed in both the optical and X-ray bands. On the ground, the wide-field 'Pi of the Sky' (PI; Ćwiok et al. 2007; Mankiewicz et al. 2014) instrument was observing, covering *Swift*'s field of view, and recorded the optical behaviour of DG CVn even before the burst began and continued until $T_0 + 1100$ s. The BOOTES-2 (Castro-Tirado et al. 1999, 2012) telescope began to observe DG CVn from $\approx T_0 +$ 11 min, starting to take spectra later at $\approx T_0 + 1$ h with the low-resolution spectrograph COLORES (Rabaza et al. 2014), covering the period of the second flare. Observations with BOOTES-2 continued for several weeks following the trigger. Deeper spectra were obtained later with instruments/spectrographs on larger telescopes: Optical System for Imaging and low-intermediate Resolution Integrated Spectrograph (OSIRIS Cepa et al. 2000) on the Gran Telescopio de Canarias (GTC) at $T_0 + 1.2$ d, Spectral Camera with Optical Reducer for Photometric and Interferometric Observations (SCORPIO; Afanasiev & Moiseev 2005) on the 6 m BTA-6

⋆E-mail: cabalma1@fel.cvut.cz
†Deceased

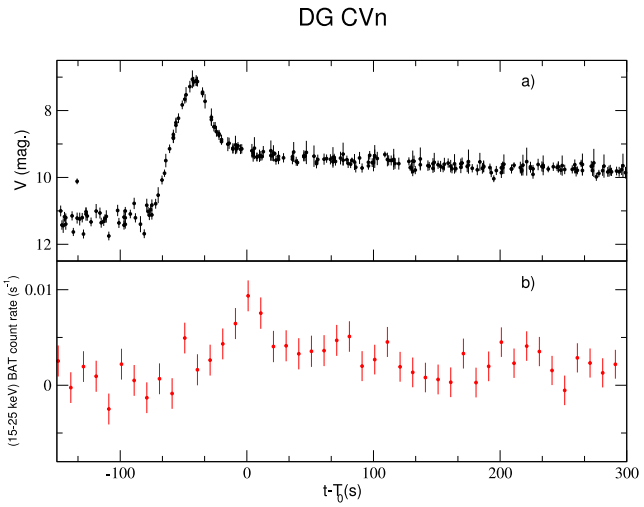

Figure 1. Hard X-ray delay versus the optical emission of the prompt emission (first flare) from DG CVn. (a) Optical light curve from the PI (from $T_0 - 150$ s onwards); (b) *Swift*/BAT light curve in the 15–25 keV energy range (i.e. hard X-rays). The time (in seconds) is measured with respect to the BAT trigger time (T_0; D'Elia et al. 2014).

telescope at Special Astrophysical Observatory (SAO) in the Caucasus at $T_0 + 15$ d and Calar Alto Fiber-fed Echelle Spectrograph (CAFE Aceituno et al. 2013) on the 2.2 m telescope at Calar Alto at $T_0 + 53$ d. Fig. 1 shows the data from the first flare: the optical light curve from PI together with the 15–25 keV *Swift* data, from $T_0 - 150$ s to $T_0 + 300$ s. Optical and X-ray observations of the second flare by BOOTES-2 and *Swift*/XRT are shown in Fig. 2.

1.1 DG CVn

DG CVn (with coordinates (J2000) $\alpha = 13^{\rm h}31^{\rm m}46\overset{\rm s}{.}7$, $\delta = 29^{\circ}16'36''$; also named G 165-8AB; Gliese & Jahreiß 1991 and 1RXS J133146.9+291631; Zickgraf et al. 2003) is a bright ($V = 12.19$; Xu et al. 2014) and close ($D = 18$ pc) visual dM4e binary system (Henry, Kirkpatrick & Simons 1994; Delfosse et al. 1998; Riedel et al. 2014). It is also a radio emitting source (Helfand et al. 1999). It has been seen that the system has Ca H&K lines in emission (Beers, Bestman & Wilhelm 1994). The components have an angular separation in the sky of 0.17 arcsec (Beuzit et al. 2004), an orbital period of $P \approx 7$ yr and magnitudes $V = 12.64$, 12.93, for the primary and the secondary components, respectively (Weis 1991; Riedel et al. 2014). It is classified as a (joint spectral type from unresolved multiples) M4.0V spectral type star (Riedel et al. 2014). It is also a red high proper motion dwarf star ($\pi \approx 80$ mas; Jiménez-Esteban et al. 2012).

One of the components of DG CVn (it is not known which one) has been reported to be chromospherically active (Henry et al. 1994) and one of the only three known M dwarf ultrafast rotators in the solar neighbourhood. The projected rotational velocity is $v \sin(i) = 55.5$ km s^{-1}, as measured from rotational broadening of the H emission lines seen in high-resolution spectra (Delfosse et al. 1998). Recently, it has been reported the detection of intense radio emission (the highest ever detected in an active red dwarf) coinciding with the time of the first and the second flares reported in this paper (Fender et al. 2015). Because the two components of the system are separated by 3.6 au ($\approx$2500 $R_\star$), the two stars are not magnetically interacting. Therefore, the intense radio emission has been interpreted as a consequence of the processes occurring in one of the

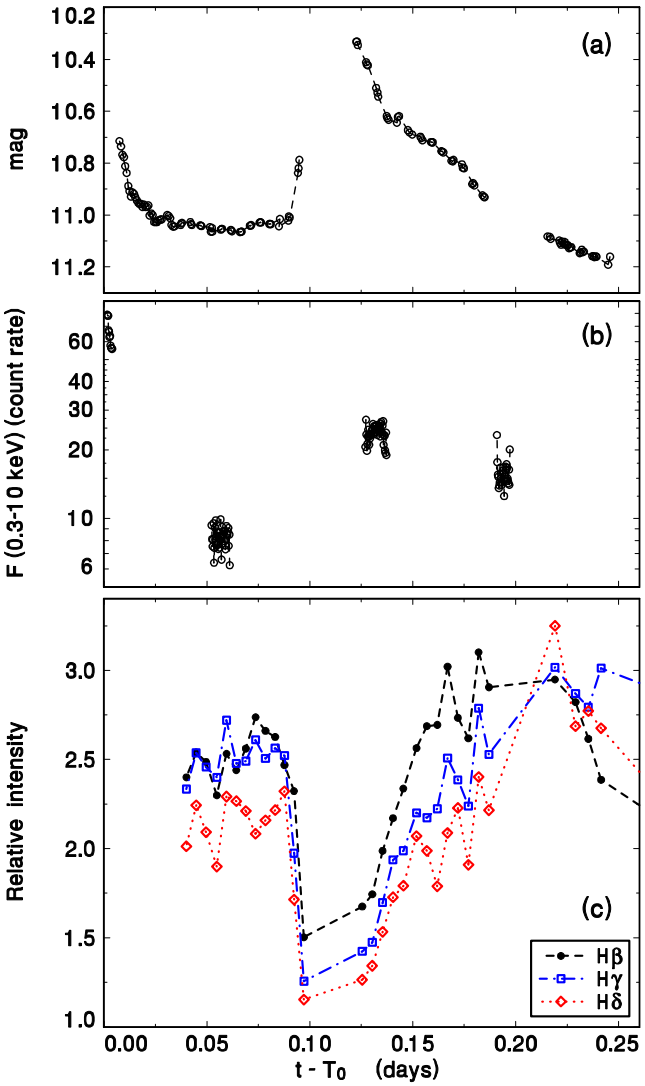

Figure 2. The X-ray brightening was accompanied by an increase of brightness of the optical continuum and the relative intensity of some spectral lines during the second flare episode. (a) Optical BOOTES-2 light curve in *V* filter during the second flare of DG CVn at $t - T_0 = 0.127$ d; (b) *Swift*/XRT light curve in the 0.3–10 keV energy range (the flux is measured in counts s^{-1}); (c) intensities of the Balmer lines (relative to the continuum) versus time obtained with the BOOTES-2/COLORES spectrograph. The uncertainties of the peak intensities are comparable to the size of the symbols. The time (in seconds) is measured with respect to the BAT trigger time (T_0; D'Elia et al. 2014).

stars (we will be referring to this as DG CVn hereafter). For this star to rotate so rapidly a tertiary close companion (i.e. apart from the distant known companion) is expected to exist, but recent studies (Fender et al. 2015) indicate that this might not be the case and that the youth of the system is the cause. Therefore, this system is considered to be a young star (30 Myr; Delfosse et al. 1998; Riedel et al. 2014). Nevertheless, it lies outside the spatial and kinematic boundaries of all known stellar young associations (Riedel et al. 2014).

DG CVn has been discovered to be an optically variable source (Robb, Balam & Greimel 1999). The light curve shows periodic sinusoidal variations with a peak to peak amplitude and photometric period of $\Delta R = 0.03$ mag and $P_{\rm phot} = 0.108\,36(2)$ d, respectively. This variation is thought to be produced by a hotspot,

whose projected area changes as the star rotates. The light curve was fitted well with a spot of approximately 3°.5 in projected radius with a temperature of 1.3 times the surrounding photosphere. This is the maximum possible value, since the effects of gravity darkening, that might be important for highly rotating stars, might have not been taken into account.

2 OBSERVATIONS

2.1 X-rays, γ-rays and optical

The BAT instrument on-board the *Swift* satellite detected a superflare from DG CVn and triggered observations at 2014 April 23, 21:07:08 UT (i.e. hereafter called T_0; D'Elia et al. 2014). During this (so-called) main flare the hard X-ray source had a peak intensity in the BAT (15–50 keV) band of ≈300 mCrab or 0.06 count cm^{-2} s^{-1}. The initial *Swift* X-Ray Telescope (XRT; Burrows et al. 2005) flux in the 2.5 s image was 4.10×10^{-9} erg cm^{-2} s^{-1} (0.2–10 keV). In the optical/UV, the source was too bright and saturated *Swift*/UVOT during the first flare (Drake et al. 2014). An optical counterpart coincident with DG CVn (and also with the X-ray source 2XMM J133146.4+291635) was identified (Xu et al. 2014) at 21:41:20 UT on 2014 April 24. Initial reports of the optical light curve indicated significant enhancement in brightness at the position of the transient and a subsequent fading of 0.92 mag h^{-1} for the first hour of observation after the peak (23:30–00:30 UT), followed by a decay rate of 0.34 mag h^{-1} for the rest 2.5 h of observation (Gazeas & Sapountzis 2014). The Major Atmospheric Gamma Imaging Cherenkov (MAGIC) telescopes started observations of the transient event at 21:08:54 UT, about 30 s after the alert was received, and kept collecting data for the next 3.3 h. A preliminary analysis gave an integral flux upper limit of 1.2×10^{-11} erg cm^{-2} s^{-1} at $E \geq 200$ GeV with a confidence limit of 95 per cent, corresponding to 5.3 per cent of the Crab nebula flux in this energy range, assuming a Crab-like spectral index (Mirzoyan 2014).

Several more smaller flares were observed with UVOT and XRT (Drake et al. 2014) after the initial trigger. They decreased in peak brightness as the overall brightness decreased. When the XRT started observing at $T_0 + 117$ s, the soft X-ray 0.3–10 keV rate of DG CVn was ≈100 counts s^{-1} and then decayed moderately, reaching a count rate of ≈50 counts s^{-1} by ≈328 s after the trigger. The soft X-ray emission had declined to a level of 4–15 counts s^{-1}, but at $T_0 + 11$ ks DG CVn was observed to have had a second, smaller flare that peaked at ≈30 counts s^{-1} in the XRT detector. We will refer to this as the second flare hereafter.

2.2 Observations with 'Pi of the Sky'

The 'Pi of the Sky' (PI) experiment is designed to monitor a large fraction of the sky with a high time resolution (10 s) and self-triggering capabilities (Ćwiok et al. 2007; Mankiewicz et al. 2014). This means that PI may be performing observations of the field of sources well before the trigger time (T_0), the latter given by high-energy instruments (like *Swift*/BAT). This approach resulted in the optical monitoring of DG CVn even before T_0. PI observed DG CVn from $T_0 - 700$ s until $T_0 + 1100$ s. In Fig. 1, the light curve is shown since ≈$T_0 - 150$ s onwards (since no significant brightness variations were detected before).

As can be seen, the optical flash only lasted about 60 s, with the source brightening by over 4 mag, to $V \approx 7$ at maximum (occurring at $t = T_0 - 41.3 \pm 0.4$ s), and ending before the maximum of the hard X-ray emission which triggered the BAT alert (T_0). Then, a slow decrease of the optical brightness was observed reaching $V = 11$ after about 0.5 h.

2.3 Observations with BOOTES

BOOTES (acronym of the Burst Observer and Optical Transient Exploring System) is a world-wide network of robotic telescopes. It was originally designed from a Spanish-Czech collaboration that started in 1998 (Castro-Tirado et al. 1999, 2012). The telescopes are located in Spain (BOOTES-1, BOOTES-2 and BOOTES-IR), New Zealand (BOOTES-3) and China (BOOTES-4). Currently, one optical spectrograph is built and working in the BOOTES network, i.e. COLORES at BOOTES-2. COLORES stands for Compact Low Resolution Spectrograph (Rabaza et al. 2014). It works in the wavelength range (3800–11 500) Å and has a spectral resolution (15–60) Å. The primary scientific target of the spectrograph is prompt gamma-ray burst (GRB) follow-up, particularly for the estimation of redshift, but it is also used to study optical transients.

COLORES is a multimode instrument that can switch from imaging a field to spectroscopy by rotating wheel-mounted grisms, slits and filters within an otherwise fixed optical system. BOOTES-2/COLORES started observing DG CVn at ≈$T_0 + 11$ min and started to take spectra later at ≈0.04 d (i.e. ≈1 h) after T_0, following the evolution of the source for several months. In this paper, we report only on the observations when the source showed emission Balmer lines (i.e. when it was 'active'). See Tables 1 and 2 and Fig. 3 for a log of the observations and the evolution of the spectra during the period of activity from the source ($t - T_0 \leq 5$ d).

BOOTES-4 observed DG CVn from $t - T_0 = 450$ s to $t - T_0 \approx 0.01$ d continuously in the clear and the Sloan g', r', i' and the United Kingdom Infrared Deep Sky Survey (UKIDSS) Z, Y filters. The best resolution achieved was 0.5 s. DG CVn showed a monotonic decrease in flux during this period. Magnitudes close to the quiescent value were obtained from $t - T_0 \approx 0.7$ d onwards.

2.4 Observations with GTC/OSIRIS and BTA/SCORPIO

We observed DG CVn with the Optical System for Imaging and low-intermediate Resolution Integrated Spectrograph (OSIRIS; Cepa et al. 2000), located at the focal plane of GTC (10.4 m), on 2014

Table 1. Log of the photometric observations reported in this work.

Obs. Date[a]	Δt[b]	Telescope/Instrument
2014-04-23 to 2014-04-23	−0.002 to 0.003	PI
2014-04-23 to 2014-04-27	0.0075 to 3.305	BOOTES-2
2014-04-23 to 2014-04-24	0.005 to 0.759	BOOTES-4

Notes. [a]The start time of an observation.
[b]The elapsed time from the start of the GRB (in days).

Table 2. Log of the spectral observations reported in this work.

Obs. Date[a]	Δt[b]	Telescope/Instrument
2014-04-23 to 2014-04-27	0.044 to 3.305	BOOTES-2/COLORES
2014-04-25	1.232 to 1.236	GTC/OSIRIS-R1000R
2014-04-25	1.233 to 1.238	GTC/OSIRIS-R2500R
2014-04-25	1.238 to 1.246	GTC/OSIRIS-R2000B
2014-05-08	14.87 to 14.88	BTA/SCORPIO-I
2014-06-15	52.99	CAHA/CAFE

Notes. [a]The start time of an observation.
[b]The elapsed time from the start of the GRB (in days).

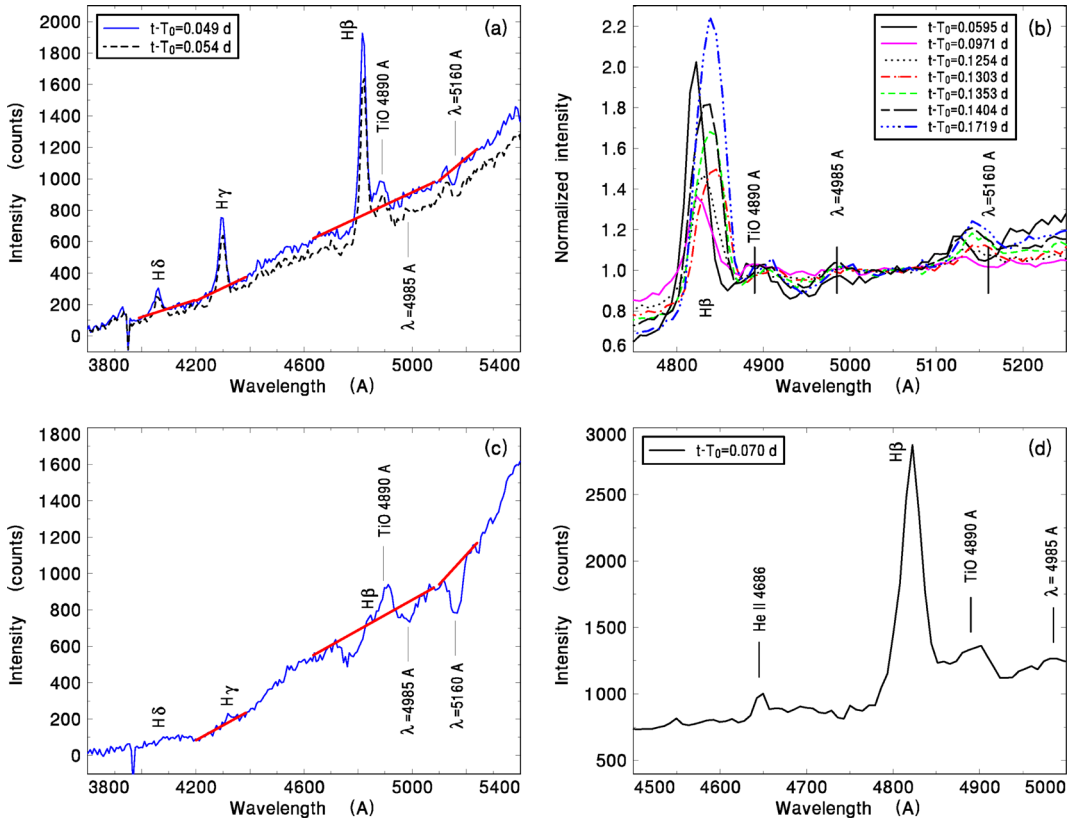

Figure 3. BOOTES-2/COLORES spectra taken before, during and after the second flare event. (a) The spectra were taken at $t - T_0 = 0.049$, 0.054 d. These show intense Balmer emission lines (H β, H γ and H δ) and some absorption–emission features at $\lambda = 4890$, 4985, 5160 Å. The regions used for the fitting of the pseudo-continuum are marked with the red line; (b) Spectra obtained during the time of the flare. Time evolution of the (relative to the continuum) intensities of the H β Balmer and transient emission line at $\lambda \approx 5160$ Å; (c) Spectrum at the late phase of the burst ($t - T_0 = 2.976$ d). Emission Balmer lines are marginally detected and the strength of the absorption features ($\lambda = 4890$, 4985, 5160 Å) has increased. The feature at $\lambda = 5160$ Å underwent a large change in time – from a blue-wing emission and a shallow absorption (panel a) to a gradual increase of absorption which even replaced the emission line (panel c). This line was in a deep absorption in the following nights. The intensity is normalized to unity at $\lambda = 5050$ Å in panel (c). (d) Spectrum showing the He II (4686 Å) emission line taken close to the time of the second flare ($t - T_0 = 0.07$ d).

April 23 (see Table 1). We used three grisms with three different spectral resolutions, i.e. R1000R, R2500R and R2000B. The blue spectra, R2000B, cover the (3950–5700) Å energy range and intense Balmer emission lines can be seen (H β,H γ,H δ and H ϵ) at (4861, 4341, 4102, 3970) Å, respectively.

In the OSIRIS red spectra, the R1000R and R2500R grisms cover the energy ranges (5100–10 000), (5575–7685) Å, respectively. They are very similar to the spectra obtained with BOOTES-2/COLORES, with the most noticeable features being the presence of molecular absorption bands and the intense H α emission line, at ≈6563 Å, typical for the spectra emitted by 'active' late spectral type stars.

We also obtained a medium–high spectral resolution spectrum with the Spectral Camera with Optical Reducer for Photometric and Interferometric Observations (SCORPIO; Afanasiev & Moiseev 2005), mounted on the BTA (6 m) telescope from the-SAO on 2014 May 8. Less intense Balmer emission lines can be seen. This indicates that the source still maintained a (low) level of activity at this time.

2.5 Observations with CAHA/CAFE

We observed DG CVn with the CAFE, located at the focal plane of the Calar Alto (CAHA) (2.2 m) telescope, on 2014 June 15 (see Table 2). This is a high ($R \approx 62\,000 \pm 5000$) resolution spectrograph working in the (3960–9500) Å) wavelength range. The spectral resolution is <0.01 Å.

The high-resolution spectrum of DG CVn during 2014 June 15, at the 2.2 m CAHA (+CAFE), contains plenty of absorption lines (mainly TiO bands), with few emission lines. The only instances of significantly broad (absorption) lines are cited in the following. Balmer lines are not seen either in absorption or in emission. Indeed, the spectrum is typical of a cold late-type ('non-active' at that time) star. There are prominent broad absorption lines at 7970–8010 Å, that dominate the spectrum in this energy range. They correspond to VO molecular transitions. These molecular transitions appear only for late-type M dwarf stars (M7 or later; Keenan & Schroeder 1952; Kirkpatrick, Henry & McCarthy 1991). Therefore, the red-dwarf might be smaller than previously considered. Nevertheless, a proper spectral classification of the emitting star on the basis of the observed high-resolution spectral features is out of the scope of this paper.

We observe at 8662 Å the Fe I doublet in absorption. The presence of this doublet is indicative of a late spectral type star in a 'non-active' state at that time. This absorption doublet line disappears when the star turns activity on, due to the chromospheric heating produced during the stellar flares (Martín 1999). The activity of DG CVn is greatly diminished during our CAFE

observations and this translates into deeper Fe I and absorption lines in general.

3 RESULTS

3.1 Optical and X-ray emission during the first flare

The delay of the initial peak of the X-ray emission (*Swift*/BAT in the 15–25 keV energy range) with respect to the peak in the optical is clearly seen in Fig. 1. We ascribe these observations to the so-called Neupert (1968) effect, observed before (apart from the Sun) in UV Ceti and Proxima Centauri (Güdel et al. 1996, 2002, 2004) with radio and X-ray observations of normal stellar flares. From the Sun and these stars it was seen that the X-ray light curve is observed to follow approximately the time integral of the *V*-band emission (radio emission in the case of the Sun). The interpretation is given in the framework of the *chromospheric evaporation* (Neupert 1968), i.e. high-energy electrons travel along magnetic fields, where the high-pitch-angle population emits prompt gyrosynchrotron emission and the low-pitch-angle population impacts in the chromosphere to produce prompt radio/*V*-band emission. The hot thermal plasma (soft X-rays) evolves as a consequence of the accumulated energy deposition, hence the integral relation. The novelty in our case is that this relationship is observed to happen in the hard X-ray emission as well, contrary to previous expectations.

In the *chromospheric evaporation* the soft X-ray emission is a signature of the thermal emission from the heated plasma. This plasma is heated after the impact by the accelerated particles, that are responsible for the early optical/radio-emission. Therefore, the detection of hard X-ray emission following the integral of the impulsive optical emission is something unexpected. This indicates that, contrary to what has been previously understood, either the plasma heats-up to $E \geq 15$ keV or that the particles emit radiation following a non-thermal kinetic distribution.

3.2 Optical spectroscopic observations

In the following, we report on the optical spectroscopic observations performed with BOOTES-2/COLORES from the beginning of the second flare (approx.) onwards. The optical spectrum from DG CVn is characterized by a strong and variable red continuum with broad molecular TiO, Ca I, Mg I, Na I absorption lines/bands superimposed. There are also intense Balmer emission lines. We notice that the intensities of the lines reported in this paper are not absolute fluxes, but relative values with respect to the continuum. To calculate the relative intensities reported in this work, local continuum segments were taken at $\lambda = 3990$–$4195, 4200$–$4385, 4635$–$5080, 5100$–5240 Å for each Hβ, Hγ and Hδ emission Balmer line, respectively. We label the continuum calculated from these segments 'pseudo-continuum', since it is not the true continuum, because it is very much affected by absorption band features in the spectrum (not constant a priori). We considered these Balmer emission lines to be excellent indicators of the spectral variability compared to the Hα line. We did this in order to avoid possible effects due to (minimal) saturation, because the Hα line was very bright. The 'relative' intensity of these lines (with respect to the continuum) is variable with time, showing a constant 'plateau' during the early phase of the burst ($t - T_0 \leq 0.10$ d), with the exception of a 'depression' (i.e. broad minimum at $t - T_0 \approx 11$ ks) that coincides both in time and duration with the second flare event (Fig. 4). After the 'plateau', the (relative) intensity of the Balmer lines progressively decreased with time until $t - T_0 \approx 3$ d. Eventually, they

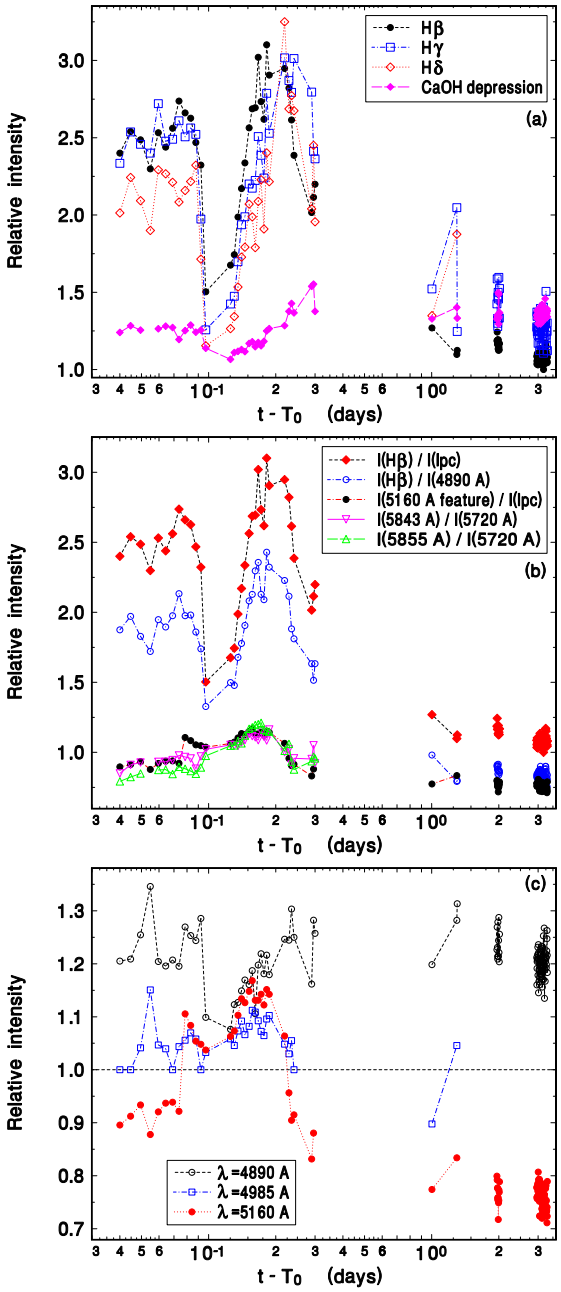

Figure 4. Evolution of the (relative to the continuum) line intensities of the BOOTES-2/COLORES spectra, fully covering the second flare event. (a) peak intensities of the Balmer lines measured with respect to the local pseudo-continuum. These Balmer lines appear in strong emission shortly after T_0 and this emission decreases in the next days. There is a minimum of Balmer line emission at $t - T_0 \approx 0.12$ d, coinciding with the time of the second smaller flare event. CaOH depression was the deepest near $t - T_0 = 0.13$ d and it was the shallowest near $t - T_0 = 0.3$ d; (b) the time evolution of the peak intensities of Hβ and the $\lambda = 5160$ Å emission feature are similar although the transient decrease of the relative intensity at $t - T_0 \approx 0.12$ d is considerably smaller for the $\lambda = 5160$ Å feature. The time evolution of the relative intensity of Hβ is mutually similar no matter if it is related to the local pseudo-continuum or to the $\lambda = 4890$ Å feature (justifying that the local continuum is a good measure of the relative intensity of the line); (c) time evolution of the intensities of several spectral features (measured with respect to the local continuum). These features vary less than Balmer lines. The uncertainties of the peak intensities are comparable to the size of the symbols.

remained minimally oscillating around a mean value close to unity (i.e. the continuum flux level).

The long-term evolution of the spectrum can be roughly characterized by the decrease of the intensity of the Balmer emission lines. At the early stage of the burst ($t - T_0 \leq 3$ d), these lines are prominent and clearly visible in the spectrum. These lines show that the star is chromospherically 'active' at the moment they are present. Eventually ($t - T_0 > 15$ d), these lines disappear and the spectrum becomes emission-featureless. This is the typical spectrum of a 'non-active' cold red-dwarf star.

But apart from the intense Balmer emission lines and broad molecular bands there are further weaker absorption and emission lines. We based our identification of these lines on the similarities with those shown in the spectra from cold red-dwarf stars (Pettersen, Cochran & Barker 1985). We find a number of spectral line features, at $\lambda = 4890, 4985, 5160$ Å. The first and the second are emission-like and the third shows an emission+absorption-line feature. After looking in more detail into the time evolution of the $\lambda = 4890$ Å emission-like line we realized that this feature is close to the boundary of the TiO absorption band. The feature at $\lambda = 4985$ Å looks like a weak emission that is only sometimes present. The $\lambda = 5160$ Å feature is often seen in absorption but sometimes it looks like a combination of absorption line and emission on its blue wing. These two lines correspond to TiO (4985 Å) and MgH+TiO (5160 Å) absorption bands, when compared with the higher resolution OSIRIS R2000B spectra taken during the 3rd day of BOOTES-2 observations. Nevertheless, still marginal residual emission at 5160 Å is seen in the OSIRIS R2000B (we will discuss this feature hereafter). Also time evolution of the CaOH depression (at $\lambda = 5530$ Å) is shown in Fig. 4. The presence of the CaOH depression is a way to distinguish normal M stars from Me (emission) stars (Pettersen et al. 1985). The CaOH depression was weaker in the early phase of the burst ($t - T_0 \leq 0.1$ d) and then it increased in the late phase ($t - T_0 > 0.2$ d). A wider broad dip minimum in the strength of the CaOH similar to that seen for Balmer lines at $t - T_0 \approx 0.12$ d is also observed for CaOH.

In Fig. 4, we show that both Hβ line and the CaOH absorption band decrease in relative strength at the time of the second flare. The time evolution of the Balmer lines and the CaOH absorption line are correlated during the early phase of the burst $t - T_0 \leq 0.2$ d. Close to the end of the burst, the Balmer emission lines become marginal and the CaOH absorption band maximal. We will discuss hereafter that both CaOH and Balmer lines features are good tracers of the behaviour of the continuum from the source. In Fig. 4, we show that the line at $\lambda = 4890$ Å (TiO) is the least time variable feature. We have checked whether this feature could be a good indicator for the local continuum taken around Hβ and found similar values to those obtained when using the local pseudo-continuum. This makes us confident on our choice of the local continua when calculating line (relative) intensities.

There are also transient emission features in our spectra at $\lambda \approx 5160, 5850, 4647$ Å. These lines are compatible with blueshifted Mg I, He D3 and He II (at $\lambda = 5183, 5876, 4686$ Å, respectively). They are blueshifted by ≈15 Å (≈37 Å in the case of He II), i.e. the same amount of shift as the Hα line (as shown hereafter), thus indicate chromospheric origin like the Balmer emission lines. Indeed, these lines have been seen during solar total eclipses (Voulgaris et al. 2010), supporting their chromospheric origin. Also, the 5876 Å line appears in emission in very strong solar flares (Johns-Krull et al. 1997 and references therein). Apart from this, these transient lines are absent during most of our spectral observations. Namely, these lines show an increase of their intensity during $t - T_0 \geq 10$ ks, coinciding with the time of the second flare event (see Fig. 3). During the rest of the time the 5160 Å feature becomes purely an MgH+TiO absorption feature. We will discuss on the importance of these transient emission features hereafter.

3.3 Shifts of the Hα line

Looking into the COLORES red spectra of DG CVn (in a period out of X-ray activity) in more detail, we see that the emission Hα line is shifting and we can tentatively see that it has a double-peaked profile. This is better seen in the higher resolution OSIRIS (Fig. 5) and SCORPIO spectra. The Hα line shows a complex P-Cyg profile, with two emission components neither of which are centred at the nominal centre of an Hα emission line. The brightest and the faintest peaks are red and blueshifted by variable amounts, with the centre of the lines moving in the (6572–6579) Å and (6548–6555) Å wavelength ranges, respectively. The centre of the complex (i.e. absorption component) of the two lines is static (6 563 ± 1)Å, coinciding with the centre of the Hα emission line at rest.

The double profile Hα has ≈15 Å redshifted and a blueshifted components. If we interpret these shifts as moving material around DG CVn, it would be moving in and out of the star at a speed of 500 km s^{-1}. This is far greater than the previously measured rotational speed of the star (i.e. 50 km s^{-1}) and indicates the likely presence of important chromospheric activity. Additionally, the stationary absorption line corresponds to photospheric absorption from the surface of the active star. Unfortunately, neither Hβ, Hγ nor Hδ show the same effect, due to their lower intensities.

Previous studies observed a solar flare with high-resolution spectroscopy found that the Hα emission line during the flare was also double-peaked during flaring activity periods (Johns-Krull et al. 1997). As in our case the line was also asymmetric, with the red wing having more emission than the blue. This effect was interpreted as redshifted emission coming from chromospheric condensations and falling towards the photosphere, or else as blueshifted absorption coming from optically thin material and rising towards the corona. They found broad emission Hα line profiles (≈100 km s^{-1}). In our case the line profiles are broader (≈500 km s^{-1}), indicating the presence of a more extreme/powerful flare event giving rise to them.

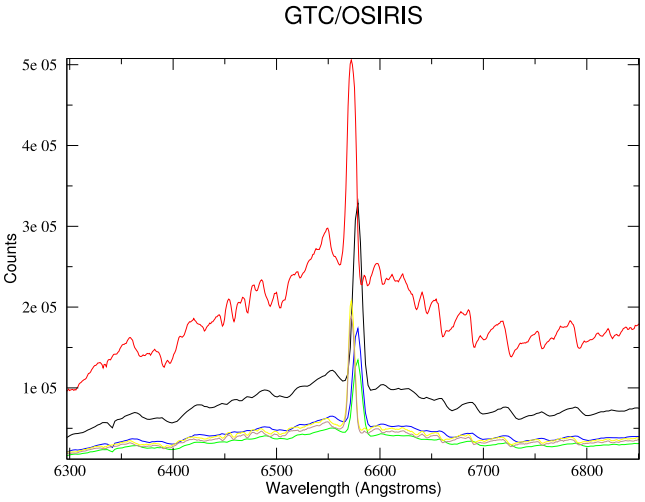

Figure 5. GTC/OSIRIS spectra from Obs. 1–6 measured from the data taken on the 2014 April 25 night (in black, red, green, blue, yellow and brown, respectively).

4 DISCUSSION

4.1 On the estimation of the age of the system

The age of DG CVn still has not been well established. Originally, it was estimated to be between the ages of the stellar associations β − Pic (12 Myr) and AB Dor (125 Myr), based on its gravity measurement and deblended H–R diagram positions (Riedel et al. 2014). Nevertheless, it has been considered to be a young system (30 Myr) because its membership to one of the solar neighbourhood 30 Myr associations gives the best match (Riedel et al. 2014). DG CVn and the other two fast rotators in the solar neighbourhood belong to the so-called zone 'C' of fast rotators which is a mixture of stars spanning a wide range of ages and/or spectral types (Mohanty & Basri 2003). Indeed, there is no consensus yet on the physical mechanism that causes a fraction of stars to retain rapid rotation rates compared to other stars of similar age (see Brown 2014 for a discussion on possible physical scenarios).

To give a further insight into the age of DG CVn, we have computed non-stop evolution models from the PMS (pre-main sequence) to WD (white dwarf) cooling sequences for two masses: 0.2 and 0.3 $M_{\odot}$. These masses are typical for red dwarfs with spectral types between M4V and M3V (Kaltenegger & Traub 2009). The calculations were performed using the MESA code (Paxton et al. 2011; Claret 2012). We adopted an initial chemical composition around the solar value ($X = 0.70, Z = 0.02$) and a mixing-length parameter $\alpha_{\rm MLT} = 1.89$. The commonly accepted age of 30 Myr is neither compatible with main sequence nor near zero-age main-sequence (ZAMS) models since the corresponding radii are too large and the star would be still in the PMS phase. However, if we assume that DG CVn contains a star which is at the ZAMS or near it, we find that the radius agrees, within uncertainties, with those tabulated (Kaltenegger & Traub 2009). The inferred age in this case is about 150 Myr for typical M4V spectral type ($\geq$150 Myr if the star is more evolved than ZAMS). The same conclusions are inferred for a star of spectral type M7V or later. We notice that the previously reported age (30 Myr; Riedel et al. 2014) is not wrong and agrees with our estimation only if we consider that it is the age of the system after achieving the ZAMS (which usually takes a time of $\approx$100 Myr of gravitational contraction from the original stellar cloud).

4.2 Conclusions

In this paper, we have studied the spectral evolution of DG CVn during an episode of important optical and hard X-ray activity. During this period at least two flares have been detected to occur quasi-simultaneously in both energy bands. We have explained the origin of the (few tens of seconds) hard X-ray delay with respect to the optical emission (Fig. 1) by the Neupert effect, which was observed before (apart from the Sun) in UV Ceti and Proxima Centauri during normal soft X-ray flares. The novelty of our study is that we observe this effect, but for the hard X-ray emission. The X-ray luminosities during the peaks of emission are $L_X(0.3–10)\,\mathrm{keV} = 1.4 \times 10^{33}$, $3.1 \times 10^{32}\,\mathrm{erg\,s^{-1}}$. Although the flare X-ray luminosities are certainly high similar values ($L_X(0.3–10)\,\mathrm{keV} \geq 10^{32}\,\mathrm{erg\,s^{-1}}$) have been detected for a dozen of cases in main-sequence red-dwarf stars. Recently, these values have been superseded by an intense episode of activity from the red-dwarf binary system SZ Psc (Drake et al. 2015). Also the duration of the flaring episode is no exception, with similar values reported for the (9 d) flare of CF Tuc observed by Kurster & Schmitt (1996) and the previous superflare from EV Lac (Osten et al. 2010). Such episodes of increased X-ray/optical activity have never been observed in the Sun so far. However, the same physics underlying the giant X-ray/optical solar flares serves to explain the superflares observed in active-like stars (as DG CVn; Aulanier et al. 2013). Nevertheless, since the most powerful solar flares have been of only about $10^{32}\,\mathrm{erg\,s^{-1}}$ (Carrington 1859) the scale-up of solar flares models would require enormous star-spots (up to 48° in latitude/longitude extent) to match stellar superflares, thus much bigger than any sunspots in the last four centuries of solar observations. Therefore, Aulanier et al. (2013) conjecture that one condition for Sun-like stars to produce superflares is to host a dynamo that is much stronger than that of the Sun. It is also worth to mention that some recent studies (Candelaresi et al. 2014; Kitze et al. 2014; Wu, Ip & Huang 2015) point out to both the (possible) few instances and the possibility of solar-type stars undergoing superflares with luminosities as high as 10^{35}–$10^{37}\,\mathrm{erg\,s^{-1}}$ under certain conditions, by using data from the *Kepler* satellite (Koch et al. 2010).

In our work, optical spectral observations began one hour after the onset of the burst, thus allowing a detailed study of the spectral properties of DG CVn during the evolution of the second flare. Balmer emission lines are prominent during the whole period of activity of the star. The optical spectra are similar to the spectra emitted by 'active' late spectral type stars. A significant decrease in the (relative to the continuum) intensity of the Balmer lines is observed during the second flare (Fig. 2). Balmer lines represent the formation and evolution of the optically thin medium above the stellar photosphere (i.e. the chromosphere). On the other hand, the variable strengths of the CaOH and TiO features represent the variations of the photosphere of DG CVn itself (where the absorption lines and the continuum emission are thought to come from). The Balmer and CaOH depressions are due to an increase of the continuum emission as well. The presence of absorption bands is due to the molecules present in the photosphere of DG CVn. As the continuum level increases the (relative to the continuum) strength of the Balmer lines and the CaOH absorption band decreases, as observed during the second flare. Therefore, the decrease of intensity of these spectral features is not real, but an artefact of an increase of the surrounding continuum.

It is in the chromosphere where the Balmer and the rest of emission lines originate. The chromosphere is more tenuous and hotter than the photosphere. Therefore only emission lines from light elements can be seen, except in the coronal transition region, where the high temperatures can ionize Fe. An increase in the intensity of the Mg I (5183 Å), He D3 (5876 Å) (and He II; 4686 Å) emission lines have been detected during the second flare of DG CVn. This indicates a correlation between the photospheric and the chromospheric activity. In other words, a change in the properties of the continuum is related to properties of the chromosphere of the red-dwarf star. We will discuss in the following on the most likely origin of this change.

The superflare observed from DG CVn during 2014 April may correspond to an episodic high-intensity flare event from a red-dwarf star. This flare event is originated from one or more active regions on the star. If there is only one active region giving rise to the observed flaring activity this star would be spinning very rapidly, with a period of a few hours ($P_{\rm rot} \approx 2.5$ h), thus giving rise to the optical phenomenology observed. Photometric studies of DG CVn performed earlier have revealed a periodicity of $P_{\rm phot} = 0.108\,36(2)$ d (Robb et al. 1999). Indeed, Robb et al. (1999) claimed that a hotspot model fit their single-band data best. This period is very close to the elapsed time between the first and the second flares, which might argue in favour of one hotspot being the responsible

for both flares. Nevertheless, the presence of a second active region (responsible for the second flare) cannot be discarded. Indeed, many active stars have active regions separated by 180° in longitude. This would 'double' the rotational period of the star. Also, given that rapidly rotating stars often have large polar spots, the lack of a dimming of the second flare due to rotational modulation might also be due to the fact that the associated active region(s) responsible for the optical flare might be also circumpolar.

Further spectroscopic and photometric observations of DG CVn would help in order to identify which is (are) the active component(s), their inclination and the actual rotation of the star. The use of spatially resolved measurements and multiband photometric data would help us to understand the exact origin of the variability.

ACKNOWLEDGEMENTS

In the memory of J. Gorosabel, for his large dedication and contribution to the study of cosmic γ-ray emitting sources of unknown origin. We thank the anonymous referee for helpful comments. This work was supported by the European social fund within the framework of realizing the project 'Support of inter-sectoral mobility and quality enhancement of research teams at Czech Technical University in Prague', CZ.1.07/2.3.00/30.0034. MCG thanks B. Montesinos, H. Krimm, T. Sakamoto and S. Pedraz for discussions. AJCT, MJ and SRO thank the support of the Spanish Ministry Projects AYA2009-14000-C03-01 and AYA2012-39727-C03-01. ACw, RO and AFZ acknowledge financial support received from the Polish Ministry of Science and Higher Education. RH acknowledges GA CR grant 13-33324S. Analysis of the data was partially based on the software developed within the GLORIA project, funded from the European Union Seventh Framework Programme (FP7/2007-2013) under grant agreement no. 283783.

REFERENCES

Aceituno J. et al., 2013, A&A, 552, 31
Afanasiev V. L., Moiseev A. V., 2005, Astron. Lett., 31, 194
Aulanier G., Démoulin P., Schrijver C. J., Janvier M., Pariat E., Schmieder B., 2013, A&A, 549, 66
Barthelmy S. D. et al., 2005, Space Sci. Rev., 120, 143
Beers T. C., Bestman W., Wilhelm R., 1994, AJ, 108, 268
Beuzit J.-L. et al., 2004, A&A, 425, 997
Brown T. M., 2014, ApJ, 789, 101
Burrows D. N. et al., 2005, Space Sci. Rev., 120, 165
Candelaresi S., Hillier A., Maehara H., Brandenburg A., Shibata K., 2014, ApJ, 792, 67
Carrington R. C., 1859, MNRAS, 20, 13
Castro-Tirado A. J. et al., 1999, A&AS, 138, 583
Castro-Tirado A. J. et al., 2012, ASI Conf. Ser., 7, 313
Cepa J. et al., 2000, in Iye M., Moorwood A. F., eds, Proc. SPIE Conf. Ser. 4008, Optical and IR Telescope Instrumentation and Detectors. SPIE, Bellingham, p. 623
Claret A., 2012, A&A, 541, A113
Ćwiok M. et al., 2007, Ap&SS, 309, 531
D'Elia V. et al., 2014, GCN Circ., 16158, 1
Delfosse X., Forveille T., Perrier C., Mayor M., 1998, A&A, 331, 581
Drake S., Osten R., Page K. L., Kennea J. A., Oates S. R., Krimm H., Gehrels N., 2014, Astron. Telegram, 6121, 1
Drake S., Osten R., Krimm H., De Pasquale M., Gehrels N., Barthelmy S., 2015, Astron. Telegram, 6940, 1
Fender R. P., Anderson G. E., Osten R., Staley T., Rumsey C., Grainge K., Saunders R. D. E., 2015, MNRAS, 446, L66
Gazeas K., Sapountzis K., 2014, GCN Circ., 16171, 1
Gehrels N. et al., 2004, ApJ, 611, 1005
Gliese W., Jahreiß H., 1991, in Brotzmann L. E., Gesser S. E., eds, Selected Astronomical Catalogs, Vol. I. NASA/Astronomical Data Center, Goddard Space Flight Center, Greenbelt, MD
Güdel M., Benz A. O., Schmitt J. H. M. M., Skinner S. L., 1996, ApJ, 471, 1002
Güdel M., Audard M., Skinner S. L., Horvath M. I., 2002, ApJ, 580, L73
Güdel M., Audard M., Reale F., Skinner S. L., Linsky J. L., 2004, A&A, 416, 713
Helfand D. J., Schnee S., Becker R. H., White R. L., McMahon R. G., 1999, AJ, 117, 1568
Henry T. J., Kirkpatrick J. D., Simons D. A., 1994, AJ, 108, 1437
Jiménez-Esteban F. M., Caballero J. A., Dorda R., Miles-Páez P. A., Solano E., 2012, A&A, 539, A86
Johns-Krull C. M., Hawley S. L., Basri G., Valenti J. A., 1997, ApJS, 112, 221
Kaltenegger L., Traub W. A., 2009, ApJ, 698, 519
Keenan P. C., Schroeder L. W., 1952, ApJ, 115, 82
Kirkpatrick J. D., Henry T. J., McCarthy D. W., Jr, 1991, ApJS, 77, 417
Kitze M., Neuhäuser R., Hambaryan V., Ginski C., 2014, ApJS, 77, 417
Koch D. G. et al., 2010, ApJ, 713, L79
Kurster M., Schmitt J. H. M. M., 1996, A&A, 311, 211
Mankiewicz L. et al., 2014, Rev. Mex. Astron. Astrophys. Ser. Conf., 45, 7
Martín E. L., 1999, MNRAS, 302, 59
Mirzoyan R., 2014, GCN Circ., 16238, 1
Mohanty S., Basri G., 2003, ApJ, 583, 451
Neupert W. M., 1968, ApJ, 153, L59
Osten R. A. et al., 2010, ApJ, 721, 785
Paxton B., Bildsten L., Dotter A., Herwig F., Lesaffre P., Timmes F., 2011, ApJS, 192, 3
Pettersen B. R., Cochran A. L., Barker E. S., 1985, AJ, 90, 2296
Rabaza O. et al., 2014, Rev. Sci. Instrum., 84, 114501
Riedel A. R. et al., 2014, AJ, 147, 85
Robb R. M., Balam D. D., Greimel R., 1999, Inf. Bull. Var. Stars, 4714, 1
Voulgaris A., Athanasiadis T., Seiradakis J. H., Pasachoff J. M., 2010, Sol. Phys., 264, 45
Weis E. W., 1991, AJ, 102, 1795
Wu C.-J., Ip W.-H., Huang L.-C., 2015, ApJ, 2015, 798, 92
Xu D., Bai C.-H., Zhang X., Esamdin A., 2014, GCN Circ., 16159, 1
Zickgraf F.-J., Engels D., Hagen H.-J., Reimers D., Voges W., 2003, A&A, 406, 535

This paper has been typeset from a TEX/LATEX file prepared by the author.